A 16-Element Subarray for Hybrid-Circuit Tile-Approach Spatial Power Combining

Mark A. Gouker, *Member, IEEE,* John T. Delisle, *Member, IEEE,* and Sean M. Duffy

Abstract—**Three designs for a 4-by-4 subarray are described for use in a spatial power-combined transmitter. The subarrays are constructed using a hybrid-circuit, tile-approach architecture and are composed of 16 cavity-backed, proximity-coupled microstrip antennas, each fed by a 0.5 watt amplifier. Both linearly and circularly polarized subarrays have been constructed for operation over a 10% band centered at 10 GHz. The linearly polarized subarray showed the following peak performance: EIRP greater than 27 dBW, effective transmitter power greater than 5 watts, dc-RF efficiency greater than 20%, and excellent graceful degradation performance.**

I. Introduction

THE EFFORTS TO develop moderate-power solid-state transmitters at microwave and millimeter-wave frequencies are increasing due to the rapid progress in transistor and integrated circuit development in recent years. To achieve moderate output power levels (tens of watts), it is necessary to combine the output from a number of transistors. There are two basic techniques to combine the outputs at these power levels: in a circuit structure, i.e., circuit power combining, or in free space, i.e., spatial power combining. In the past several years one form of spatial power combining, quasi-optical power combining, has gained considerable attention [1]–[3].

Some of the benefits of the quasi-optical approach, however, are common to all types of spatial power combining [4]–[7]. The most notable benefits are graceful degradation and the realization of significant output powers from modest size transistors. Unlike quasi-optical configurations which are spatially-fed, spatially-combined arrays, the basic configuration in this paper is a circuit-fed, spatially-combined array. The circuit-fed approach has a number of advantages. It is easier to obtain uniform amplitude and phase at each of the elements. The loss in the corporate feed network can be hidden by placing driver amplifiers in the feed. There is more latitude in choosing the circuit layout, amplifiers, and antennas to meet the system requirements.

In a previous paper, we reported on the architecture for a hybrid-circuit, tile-approach spatial power-combined transmitter [7]. This design is different from other spatial-power combining efforts in that it gives priority to the issues of thermal management, maximizing combining efficiency, and maximizing graceful degradation. In this paper we discuss the design and measured results for three different subarrays appropriate for this architecture. In a complete transmitter a number of these subarrays would be tiled into an extended array.

Manuscript received March 15, 1996; revised July 22, 1996. This work was supported by the Advanced Research Projects Agency under Contract F19628-95-C-0002.

The authors are with the Lincoln Laboratory, Massachusetts Institute of Technology, Lexington, MA 02173 USA.

Publisher Item Identifier S 0018-9480(96)07921-5.

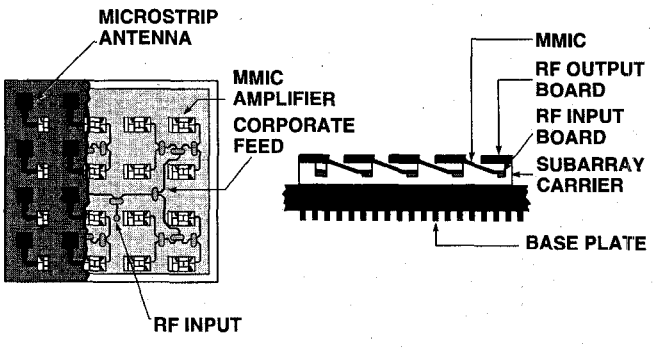

Fig. 1. (a) Top and (b) side views of the two RF-level subarray design.

II. Design

An illustration of the 4-by-4 element subarray is shown in Fig. 1. The design resembles conventional tile-approach phased arrays; however, the implementation has been tailored for the spatial power combining application. Each element consists of a monolithic microwave/millimeter wave integrated circuit (MMIC) amplifier and a proximity coupled microstrip antenna. A corporate feed network distributes the input signal to each of the MMIC amplifiers, and the output of the amplifiers is combined in free space after being radiated from the microstrip antennas.

The subarray is specifically designed to be a hybrid construction of printed circuit boards and MMIC amplifiers integrated onto a single metal carrier. The hybrid approach offers many design options not available in a monolithic approach. The MMIC amplifiers can be tested before insertion into the circuit. This insures that 100% of the amplifiers are RF good and that their large signal amplitude and phase are similar. Populating a subarray with amplifiers which have similar performance increases the combining efficiency. The hybrid approach allows the freedom of selecting a lower dielectric constant circuit board for the antenna layers to increase the radiation efficiency. The hybrid approach also allows multiple RF levels (in this case two) for increased isolation and increased circuit density.

The entire subarray is integrated on a metal carrier. The MMIC amplifiers are attached directly to the subarray carrier in order to provide a low thermal resistance path to the heat sink. Multiple subarrays can be tiled to a transmitter base plate. The base plate houses the RF and dc distribution to the subarrays, and the entire backside of the base plate is reserved for the heat sink. The low thermal resistance path from the MMIC's to the heat sink allows the possibility of using higher output power transistors than other spatial power-combining approaches while still maintaining low junction temperatures for reliable operation.

The subarray is constructed with two multilayer printed circuit boards as shown in Fig. 1. The lower circuit board contains the dc power distribution layer and the RF input corporate feed network. The top circuit board contains the microstrip antennas. The height of the air gap between the two printed circuit boards is chosen so that the field configuration of the microstrip lines in the input feed network is not perturbed much from a conventional uncovered microstrip line. This facilitates the transition into the MMIC amplifiers. The ground plane of the RF output layer acts as a shield to reduce the feedback from the field radiated by the microstrip antennas to the RF input network. An early version of the subarray, consisting of a single RF level design with input feed, amplifiers and antennas on the same layer, oscillates because of this feedback path. The two-level approach shown in Fig. 1 has sufficient isolation to prevent oscillation.

In this design, the signal is transitioned from the bottom circuit board to the top circuit board by placing the MMIC on a 10 degree ramp. Simple ribbon bonds are made at the input and output of the amplifier carrier. The ramp approach decreases the RF discontinuity but at the price of increasing the fabrication complexity. Other transition strategies include a long ribbon bond, a RF via, or a coupling aperture. These transition techniques ease the fabrication by keeping the MMIC horizontal but can introduce a significant discontinuity, especially at higher frequencies.

The input feed network is a standard 1-to-16 corporate divider. All of the dividers are Wilkinson dividers to improve the isolation between the elements. Thus, if one of the MMIC amplifiers fails, the effect on the other elements in the subarray is minimized. This added isolation aids the graceful degradation performance of the array. A photograph of the input feed layer and MMIC amplifiers is shown in Fig. 2.

The MMIC amplifiers used in these arrays are Texas Instruments TGA 8031-SCC. They have been attached to individual copper-tungsten carriers with input and output alumina microstrip boards and some filtering elements in the bias lines to insure stable operation. Placing the MMIC's on individual carriers allowed measurement of the devices before inserting them into the array. This measurement is necessary to select MMIC's with similar phase and amplitude characteristics and to measure their output power into a 50 ohm load for use in the calculation of the combining efficiency. The selected bias voltages are $V_D = 5.2$ V, $V_G = -2.3$ V, and $V_{\mathrm{CTRL}} = 0.6$ to -1.2 V. V_{CTRL} can be used to adjust the S_{21} of the amplifier. The typical performance of the amplifiers with this bias is Gain $= 32$ dB, $P_{\mathrm{OUT}} = 27$ dBm, and PAE $= 27\%$.

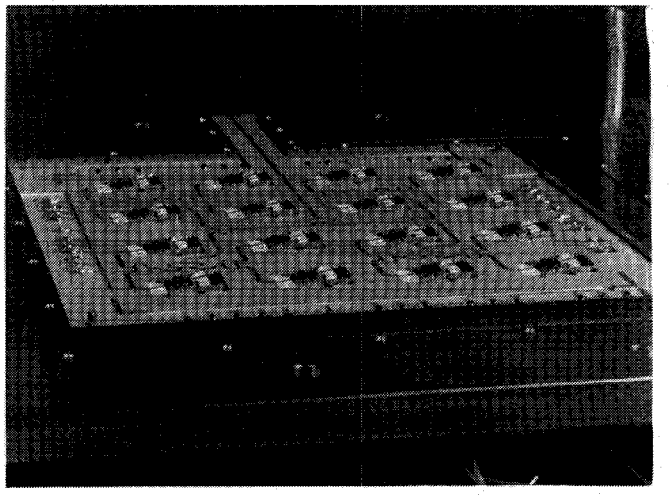

Fig. 2. Photograph of the RF input circuit board and MMIC amplifiers.

III. Cavity-Backed Antenna

The proximity coupled microstrip antennas used in this work are constructed on a two substrate-layer printed circuit board [8]. The choice of this type of microstrip antenna is driven by reserving the backside of the transmitter array for thermal management and providing a low thermal resistance path from the MMIC's to the cooling fins. This antenna has the feed line and the patch on the same side of the ground plane.

The subarrays discussed in [7] used proximity coupled antennas of a conventional design on a circuit board with dielectric constant of 2.94 (Duroid 6002). In the current work, cavity-backed, proximity coupled patch antennas are used. A diagram of the design is shown in Fig. 3. The cavity is constructed by placing a ring of plated-through holes around each patch. An additional ground plane placed on the top surface of the circuit board finishes the formation of the cavity and helps shield the feed network from the radiated signal. Constructing the cavity using plated-through holes does not complicate the fabrication since plated through holes are standard in printed circuit board fabrication.

The purpose of the cavity is to prevent the guided wave propagation in the circuit board. This has two benefits. First, it decreases the mutual coupling by eliminating the portion that travels through the circuit board. Second, the radiation efficiency of the antenna remains high because the loss to guided waves is removed [3], [9], [10]. Thus cavity-backed patches can be constructed on relatively thick, moderately high dielectric constant boards. A higher dielectric constant makes it possible to shrink the size of the distributed elements, such as power dividers and impedance transformers. The cavity-backed antenna enables the circuit boards to be constructed with high volume cofired ceramic techniques which have dielectric constants in the 6 to 7 range. These substrates offer advantages over Teflon based boards such as better control of circuit feature sizes, integrated lumped elements, easier wire bonding, and CTE closer to GaAs.

The input impedances of the cavity-backed patch antenna are controlled primarily by the dimensions of the patch and feed. As long as the cavity walls are at least a substrate height

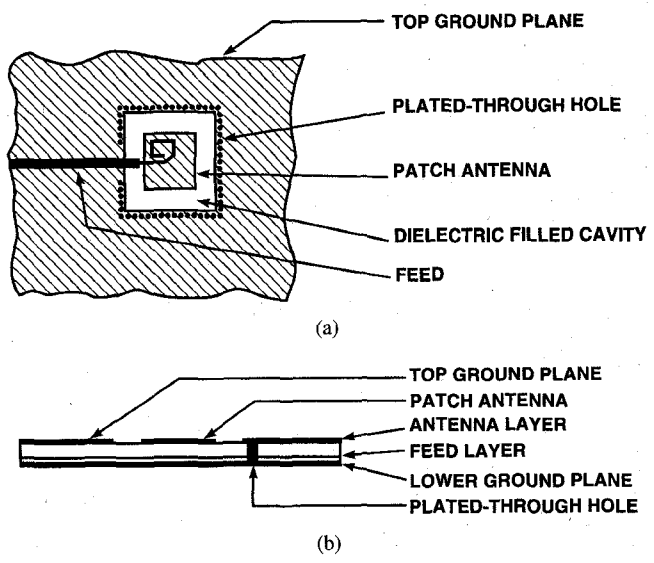

Fig. 3. Illustration of the cavity-backed, proximity-coupled microstrip antenna. (a) Top view. (b) Side view.

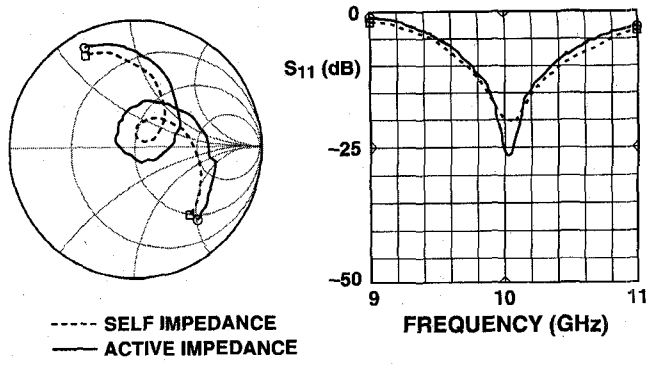

Fig. 4. Self and active impedances of the LP cavity-backed, proximity-coupled microstrip antenna.

away from the patch, the cavity does not significantly alter the impedance. The impedance locus of the patch can be tuned by altering the length and width of the feed line under the patch and by altering the ratio of feed substrate height to total substrate height. A more in-depth discussion of the cavity-backed patch antenna will be given in a forthcoming paper.

The antennas in these subarrays are constructed with Duroid 6002, largely because the design has evolved from earlier work [7]. The feed layer thickness is 0.64 mm, and the total circuit board height is 1.78 mm. The spacing between antennas is $0.8\lambda_o$. The plated-through holes are 0.64 mm in diameter and are placed on 0.89 mm centers. There are approximately 2000 plated-through holes in a 4-by-4 subarray.

The self and active impedance for a linearly polarized antenna with a quarter-wave transformer is shown in Fig. 4. The self impedance of the patch is the input impedance when the antenna is isolated. The active impedance is the ratio of reflected wave to input wave while all the antennas in the array are radiating. This is the impedance presented to the MMIC under normal operation of the subarray, and thus the impedance that must be considered for proper design of the array. In this work the active impedance was found through measurement of a 1-by-4 E-plane array. A Hewlett-Packard 8511 test set was used with appropriate power splitters, bi-directional couplers, and phase trimmers. The mutual coupling between the linearly polarized elements in the H-plane is negligible, so the E-plane 1-by-4 array is an accurate measurement of the active impedance. The curves in the figure are for one of the center elements in the array.

IV. Measured Results

Three different antenna configurations were investigated in this work, one linearly polarized (LP) and two circularly polarized (CP). Both CP designs use a power splitter to feed orthogonal sides of the patch and a $\lambda_g/4$ line length differential to achieve phase quadrature. One CP design uses a Wilkinson divider for better axial ratio performance, and the other uses a reactive T-junction divider and a diamond-set arrangement for space reduction. The layouts of these elements is shown in Fig. 5. The LP and the diamond-set CP antenna designs are such that the entire subarray fits within a $3.2\lambda_o$ $(4 \times 0.8\lambda_o)$ area. Thus these subarrays could be tiled into a larger array. The CP design with Wilkinson dividers is too large for tiling into an extended array, but it was investigated for its higher quality CP radiation.

The equivalent isotropic radiated power (EIRP) and radiation patterns were measured for all of the subarrays. The effective transmitter power, dc-RF efficiency and combining efficiency were calculated from the measured EIRP. The effective transmitter power [11] is defined as the EIRP divided by the *directivity* of the array. Using the directivity instead of an estimate of the gain of the array has several advantages. First, the directivity of the array is unambiguous. For a uniformly excited array, as in this work, the directivity can be calculated from the physical aperture. Second, the loss in the array is properly taken into account by using the directivity. The unwanted phase and amplitude variations among the array elements and the radiation efficiency of the patch antennas impact the effective transmitter power. Finally, the effective transmitted power is roughly equivalent to the measured output power of a circuit combined transmitter.

A photograph of the fully assembled LP subarray is shown in Fig. 6. The EIRP, effective transmitter power, and dc-RF efficiency for the LP subarray are shown in Fig. 7. These results are for the amplifiers operating in saturation. The EIRP peaks at 27.2 dBW at 9.7 GHz with a corresponding effective transmitter power of 5.0 watts and dc-RF efficiency of 21%. The 3 dB drop in EIRP in the center of the band is caused by insufficient isolation between the radiated field and the input feed network. While the leakage is not great enough to cause oscillations, a portion of the radiated field is still picked up by the input feed and causes interference of the input signal at the input of the amplifiers.

The combining efficiency versus frequency is shown in Fig. 8. The peak combining efficiency is 64% at 9.6 GHz. The combining efficiency is taken as the effective transmitter power divided by the sum of the available power from each of the MMIC's. The available power was measured with the MMIC on its individual carrier driving a 50 ohm load. This

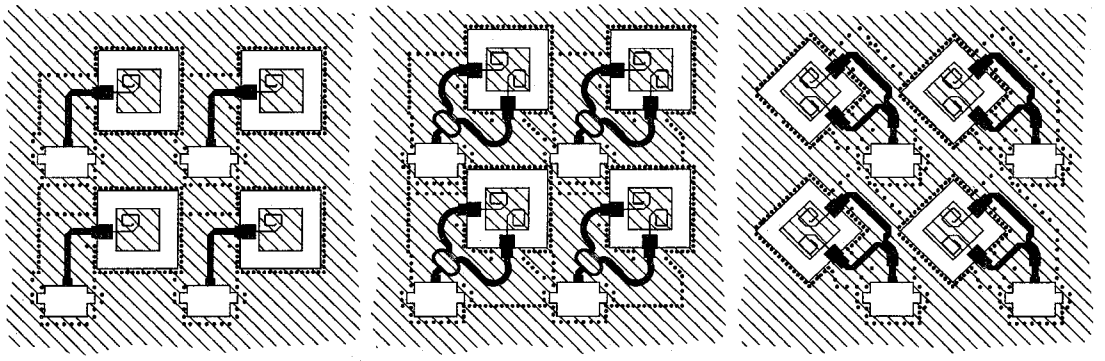

(a) (b) (c)

Fig. 5. Two-by-two illustrations of the antenna layout in the three subarrays designs: (a) LP design, (b) CP with Wilkinson dividers, and (c) CP diamond set with reactive T-junction dividers.

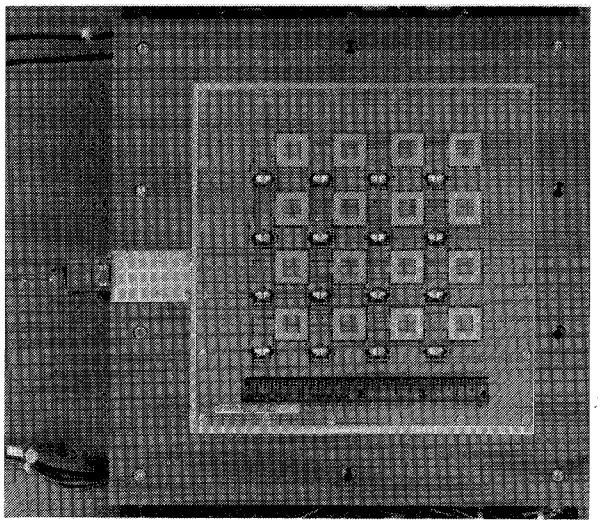

Fig. 6. Photograph of the fully assembled LP subarray.

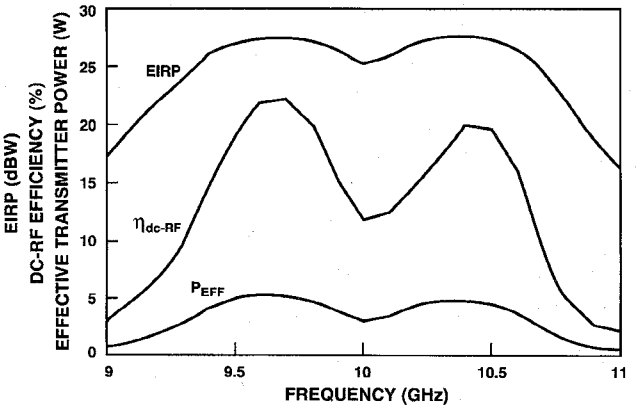

Fig. 7. EIRP, dc-RF efficiency, and effective transmitter power for the LP subarray.

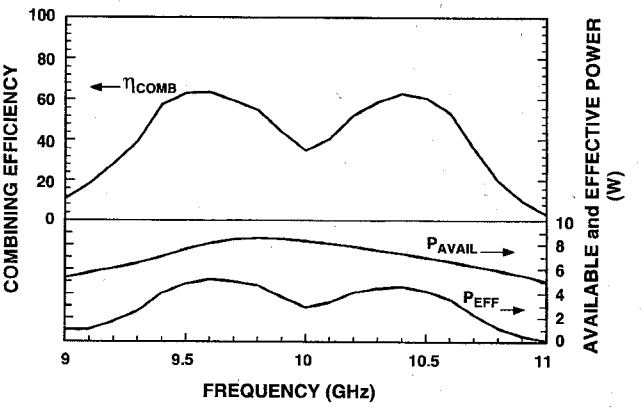

Fig. 8. Combining efficiency, available power, and effective transmitter power for the LP subarray.

is a conservative definition of the combining efficiency that includes the major loss mechanisms in the array: the imperfect feeding of the subarray, the nonoptimum load presented to the amplifiers, the radiation efficiency of the patch antennas, and the phase and amplitude variation among the array. Typical reported combining efficiencies only include loss due to phase and amplitude variations among the array elements. It is felt the definition used here more accurately reflects the system performance and provides a better comparison to the efficiency of circuit combined approaches. Far-field patterns for the subarray are shown in Fig. 9. The unevenness in the sidelobes is due to phase and amplitude variations in the array.

The measured EIRP, effective transmitter power and dc-RF efficiency for the circularly polarized subarray with Wilkinson dividers [Fig. 4(b)] are shown in Fig. 10. The EIRP peaks at 26.9 dBW at 10.1 GHz with a corresponding effective transmitter power of 4.3 watts and dc-RF efficiency of 17%. The decrease in the EIRP and the other figures-of-merit calculated from it is caused by the loss in the power divider and extra line length in the feed from the amplifier to the antenna. The measured far-field patterns for the subarray are shown in Fig. 11. The plot shows a vertical and horizontal cut of the dominant right-hand circularly polarized wave. The cross polarization cut is the left-hand CP wave. The far-field patterns for the CP subarrays were calculated from near-field measurements. The axial ratio of the radiated field was less than 2 db across a 10% band centered at 10 GHz.

The figures-of-merit for the circularly polarized subarray with reactive T-junction dividers and diamond-set arrangement are about the same as the other CP subarray. The only exception is the axial ratio of the radiated field which had a best value of 5 dB in the 10% band of interest. The poor quality CP was caused primarily from an unoptimized design,

TABLE I
SUMMARY OF PERFORMANCE FOR THE THREE SUBARRAYS AVERAGED OVER A 10% BANDWIDTH WITH NOMINAL CENTER FREQUENCY OF 10 GHz

	EIRP	Effective Tx Power	dc-RF Efficiency	Combining Efficiency
LP Subarray	27.1 dBW	4.3 W	17.2 %	54 %
CP Wilkinson	26.6 dBW	3.6 W	15.2 %	44 %
CP Diamond Set	26.5 dBW	3.6 W	14.3 %	46 %

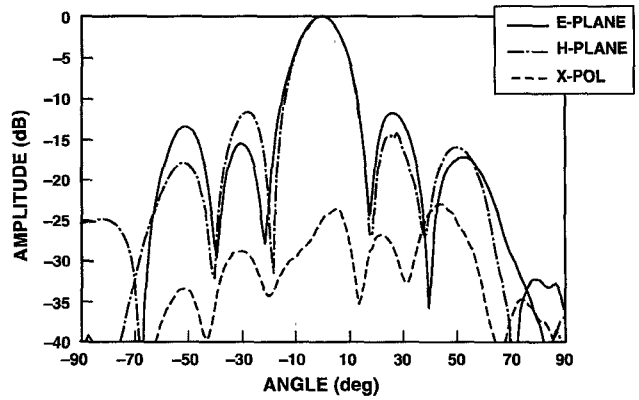

Fig. 9. Farfield patterns for the LP subarray.

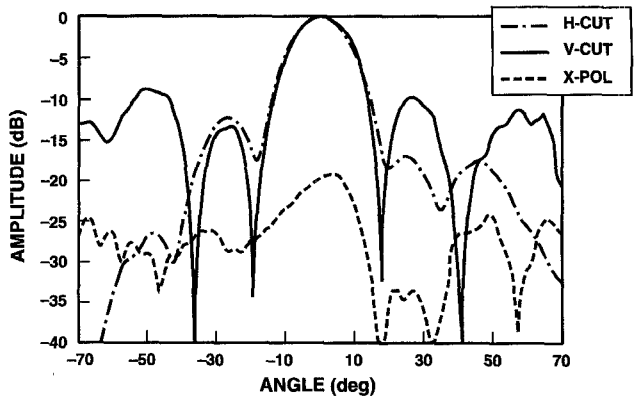

Fig. 11. Farfield patterns for the CP subarray with Wilkinson dividers.

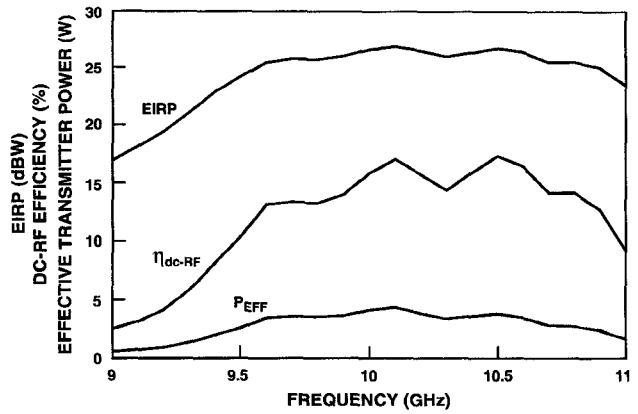

Fig. 10. EIRP, dc-RF efficiency, and effective transmitter power for the CP subarray with Wilkinson dividers.

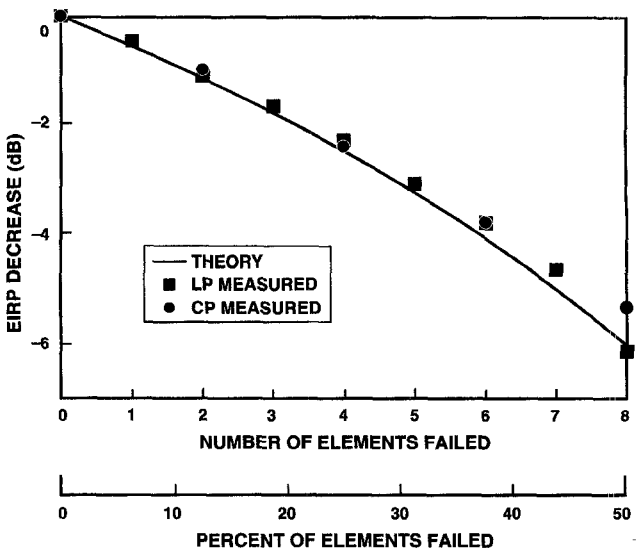

Fig. 12. Graceful degradation performance of the LP and CP subarrays.

but it also reflects that an orthogonally fed patch using a reactive T-junction requires a more precise design and has inherently narrower bandwidth than one using a Wilkinson divider. For this subarray the EIRP is calculated for the total radiated power not just the power in the desired RHCP wave. Clearly this antenna design would have to be iterated before use in a real system, but the results calculated from the total radiated power show the potential performance for an optimized antenna design.

The graceful degradation performance of the subarrays is shown in Fig. 12. The theoretical curve in the plot is the calculated decrease in EIRP based on simply removing elements from the array. Thus, it represents the maximum graceful degradation performance. The measured results were obtained by turning off random elements in the array. The agreement between the curves indicates that the input signal is not significantly changed under the failure of devices. It also indicates that the change in load impedance presented to the amplifiers which arises from the change in active impedance of the antenna is not significant for failure of up to 40% of the elements.

The results for all three subarrays are summarized in Table I. The EIRP, effective transmitter power, dc-RF efficiency, and the combining efficiency averaged over a 10% bandwidth are shown in the table. The band for averaging the LP array results is centered at 10.0 GHz while the band for both of the CP arrays is centered at 10.2 GHz. It is believed that this averaging is a fair representation of the array performance and that centering the optimum performance at the desired 10 GHz could be accomplished with further iterations of the design.

V. Conclusion

Three different designs for a circuit-fed, spatially-combined subarray have been presented. Two of these designs are appropriate for tiling the subarrays into an extended array. The measured results show EIRP's in excess of 27 dBW with corresponding effective transmitter powers of 5 watts and dc-RF efficiencies greater than 20%. The most indicative figure-of-merit, however, is the combining efficiency which peaked at 64% for the LP array. For the spatial power-combined architecture described in this paper, the combining efficiency would remain essentially constant no matter how many subarrays are tiled together. This is fundamentally different from a circuit combined approach where the combining efficiency decreases as the number of amplifiers in the system increases.

Acknowledgment

The authors would like to thank R. Magliocco, L. Hill, and S. Robertson for assembly of the arrays. They are grateful to D. Snider and R. Bauer for their continued support and encouragement.

References

[1] J. W. Mink, "Quasi-optical power combining of solid-state millimeter-wave sources," *IEEE Trans. Microwave Theory Tech.,* vol. 34, pp. 273–279, Feb. 1986.

[2] R. M. Weikle II, *et al.* "Transistor oscillator and amplifier grids," *Proc. IEEE,* vol. 80, pp. 1800–1809.

[3] R. A. York, "Quasi-optical power combining techniques," in *Millimeter and Microwave Engineering for Communication and Radar,* J. C. Wiltse, Ed., Bellingham, WA, SPIE, vol. CR54, pp. 63–97.

[4] J. Lin and T. Itoh, "A 4×4 spatial power-combing array with strongly coupled in multi-layer structure," in *IEEE MTT-S Int. Microwave Symp. Dig.,* Atlanta, GA, June 1993, pp. 607–609.

[5] J. A. Bent, *et al,* "Spatial power combining for millimeter wave solid state amplifiers," in *IEEE MTT-S Int. Microwave Symp. Dig.,* Atlanta, GA, June 1993, pp. 619–622.

[6] A. Balasubramaniyan and A. Mortazawi, "Two-dimensional MESFET-based spatial power combiners," *IEEE Microwave Guided Wave Lett.,* vol. 3, pp. 366–368, Oct., 1993.

[7] M. A. Gouker, R. G. Beaudette, and J. T. Delisle, "A hybrid-circuit tile-a pproach architecture for high-power spatial power-combined transmitters," in *IEEE MTT-S Int. Microwave Symp. Dig.,* San Diego, CA, May, 1994, pp. 1545–1548.

[8] G. Splitt and M. Davidovitz, "Guidelines for design of electromagnetically coupled microstrip patch antennas on two-layer substrates," *IEEE Trans. Antennas Propagat.,* vol. 38, pp. 1136–1140, July 1990.

[9] F. Zavosh and J. T. Aberle, "Single and stacked circular microstrip patch antennas backed by a circular cavity," *IEEE Trans. Antennas Propagat.,* vol. 43, pp. 746–750, July 1995.

[10] S. M. Duffy and M. A. Gouker, "Experimental comparison of the radiation efficiency for conventional and cavity backed microstrip antennas," presented at the *IEEE AP-S Int. Symp.,* Baltimore, MD, July 21–26, 1996.

[11] M. A. Gouker, "Toward standard figures-of-merit for spatial and quasi-optical power-combined arrays," *Trans. Microwave Theory Tech.,* vol. 43, pp. 1614–1617, July 1995.

Mark A. Gouker (S'84-M'92) received the B.S. degree in physics from Emory University, Atlanta, GA, and the M.S. and Ph.D. degrees from the Georgia Institute of Technology, Atlanta, in 1983, 1985, and 1991, respectively.

From 1985 to 1987 he was a Research Engineer at the Georgia Tech Research Institute working on millimeter-wave integrated circuit antennas. Since 1991 he has been with Lincoln Laboratory, Massachusetts Institute of Technology, Lexington, MA. His research interests are in microwave and millimeter-wave integrated circuits and antennas.

John T. Delisle, (S'87–M'89) received the B.S. degree in electrical engineering from Rensselaer Polytechnic Institute and the S.M. in electrical engineering from the Massachusetts Institute of Technology, Lexington, MA.

He has been with MIT Lincoln Laboratory since 1991 where he currently designs microwave and millimeter wave circuits for EHF satellite ground terminals.

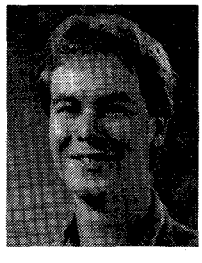

Sean M. Duffy, received the B.S. and M.S. degrees in electrical engineering from the University of Massachusetts, Amherst, in 1993 and 1995, respectively, and is currently working toward the Ph.D. degree there.

Since 1995 he has been with MIT Lincoln Laboratory, Massachusetts Institute of Technology, Lexington, MA. His current research interests are in the design and analysis of printed antennas and millimeter wave multichip modules.